STATUS OF THE INP OPTICAL KLYSTRON

G.A. KORNYUKHIN, G.N. KULIPANOV, V.N. LITVINENKO, N.A. MESENTSEV, A.N. SKRINSKY, N.A. VINOKUROV and P.D. VOBLYI

Institute of Nuclear Physics, 630090, Novosibirsk, USSR

The result of recent experiments with the optical klystron OK-2 installed in the storage ring VEPP-3 are presented. The current status, the new magnetic system design OK-3, and some prospects and plans are described.

1. Introduction

Since 1979 the study of the optical klystron, proposed in our Institute, is under way in the storage ring VEPP-3. The optical klystron (OK) differs from the conventional free electron laser [1–4] in having a much higher gain. The first version of the optical klystron magnetic system (OK-1) was used in the study of the spontaneous radiation spectrum [2] in 1979, and in the gain measurements in 1980 [4,5]. An improved second version of the magnetic system OK was manufactured in 1981, OK-2 [4,6], providing a higher gain per pass.

In the spring of 1980 work started to obtain lasing in OK. This work continued until the middle of July 1982.

2. Magnetic system of the storage ring VEPP-3

The storage ring VEPP-3 consists of two half-rings with a mean radius of 8 m, each connected by straight line sections 12 m long. In each straight section there are four doublets, connected in series. In one of the sections the injection system and two RF-cavities are installed: one on the first harmonic of the revolution frequency ($q = 1$, $f = 4.03$ MHz, $V = 8$ kV), the second with $q = 19$, $f = 76.6$ MHz, $V = 600$ kV. In the center of

the other section the magnetic system of the optical klystron was installed (see fig. 1). Here four magnets produced a compensated distortion of the orbit and put the beam into the narrow part of the vacuum chamber. This section of the vacuum chamber had been used earlier for operation with the superconducting snake. It has some serious disadvantages: (i) the free length for the OK magnetic system was only 1.1 m; (ii) the vacuum chamber was made of stainless steel with $\mu = 1.5$ which caused a strong inhomogeneity in the magnetic field.

The work with the OK was carried out at the energy of injection $E = 350$ MeV. In the standard mode of the VEPP-3 operation the section matrices are unity and the betatron frequencies are $Q_x = 5.17$, $Q_z = 5.13$. To readjust the storage ring we used the distributed F and D gradient correctors in the half-rings, making the section matrices slightly different from unity. The change of the VEPP-3 magnetic system was required to decrease the values β_x and β_z down to $\beta_x = 1.5$ m and $\beta_z = 0.8$ m and to make the transverse dispersion equal to zero ($\eta = 0$, $\eta' = 0$) at the location of the magnetic system. This enabled an acceptable capture efficiency and beam lifetime in spite of large inhomogeneities of the field. In addition, operation with $\eta = 0$ and $\eta' = 0$ was necessary for a fine tuning of the distance between the mirrors of optical cavity (see sect. 4).
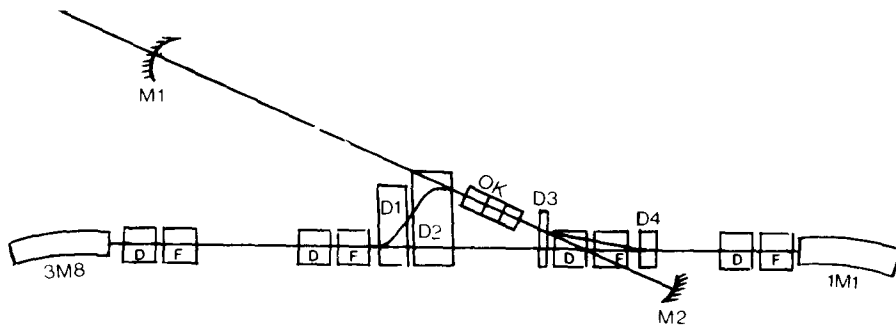

Fig. 1. Scheme of OK magnetic system installed in VEPP-3.

Table 1
Beam parameters of the storage ring VEPP-3 during the operation with the optical klystron

Circumference of equilibrium orbit	$P = 74.4$ m
Energy	$E = 350$ MeV
Energy spread	$\sigma_E/E = 4 \times 10^{-4}$
Beam dimensions and angular spread at the OK magnetic system	$\sigma_x = 0.2$ mm, $\sigma_z = 0.1$ mm $\sigma_{x'} = 5 \times 10^{-4}$, $\sigma_{z'} = 4 \times 10^{-4}$
Bunch length	$\sigma_l = 3.5$ cm
	($q = 19$; $V = 100$ kV; $I = 0.3$ mA)

3. Beam parameters in the storage ring VEPP-3

The beam parameters in the storage ring VEPP-3 at an injection energy $E = 350$ MeV for small currents have been measured earlier [13]; they are given in table 1. During operation substantial variations of the beam parameters were observed with increasing current. With the 4 MHz ($q = 1$) cavity switched on and with the 76 MHz ($q = 19$) cavity strongly mistuned, the typical Touschek increase of energy spread was observed (see fig. 2):

$$\sigma_E \sim I^{1/6}.$$

With currents of our interest, ~ 20–30 mA, the bunch length (at voltage $V = 7.5$ kV) was $(2\pi)^{1/2}\sigma_l = l = 1.6$ m. In order to increase the peak current, $I_{peak} = \bar{I}P/l$, to which the OK peak gain is directly proportional, the bunch length was decreased by the use of the 76 MHz ($q = 19$) cavity. In this case turbulent bunch lengthening is observed with increased peak currents, apparently due to beam interaction with one of high frequency longitudinal modes of the cavity. According to our measurements the energy spread dependence on the current is well described by the following formula (see
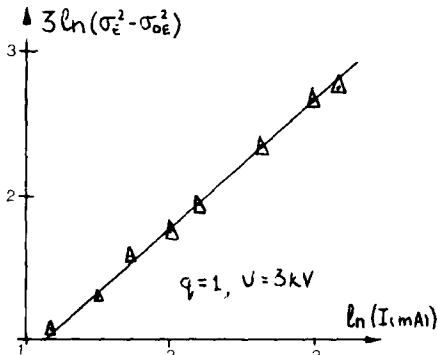
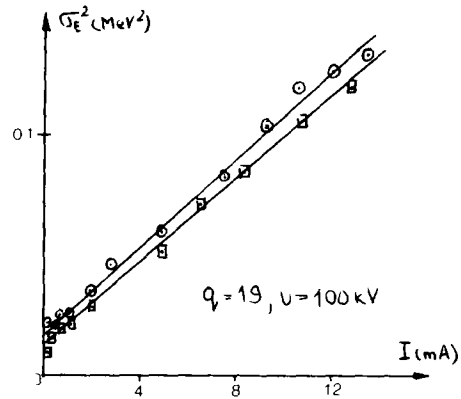Fig. 2. Energy spread as a function of current ($q = 1$, $V = 3$ kV).

Fig. 3. Energy spread as a function of current ($q = 19$, $V = 100$ kV): □ from the bunch length measurement, ⊙ on the spontaneous radiation spectrum.

fig. 3):

$$\frac{\sigma_{E}^2 - \sigma_{E_0}^2}{E^2} = \frac{\bar{I}}{I_0} V_{19}^{1/2} \text{ (kV)}, \tag{1}$$

where $\sigma_{E_0} = 0.13$ MeV is an energy spread at small current, and $I_0 = 4.1 \times 10^5$ A from our measurements.

4. Optical cavity of the klystron

The OK optical cavity consists of two multi-layer dielectric mirrors (see fig. 1) with reflection maxima at wave length $\lambda_0 = 6300$ Å. The forward mirror (M1), which is affected by direct radiation from OK magnetic system, has a curvature radius $R_1 = 5.8$ m and a diameter of 40 mm. The curvature radius of the rear mirror (M2) is $R_2 = 4$ m, and its diameter is 20 mm. The distance between the mirrors is one eighth of the storage ring circumference: $L = 9.3$ m. The mirror radii are chosen in such a way that the minimum size for the main mode of the optical cavity is at the same place where the OK magnetic system is installed, i.e. in the interaction region. The light "β-function" here is equal to 1.1 m

$$\beta_r^2 = \frac{L(R_1 + R_2 - L)(L - R_1)(L - R_2)}{(2L - R_1 - R_2)^2}.$$

The transverse radius of the light beam is $\sigma_r = (\lambda\beta_r/2\pi)^{1/2} = 0.33$ mm and the effective area of transverse cross section is $S_{eff} = \lambda\beta_r/2 = 0.35$ mm^2. The transverse dimensions of electron beam are smaller than σ_r, and consequently, the OK gain does not depend on the beam size.

The optical cavity alignment was performed in two stages. The mirrors were first installed into the vacuum chamber with an accuracy of ~ 1 mm and ~ 3 mm in

the transverse and longitudinal direction, respectively. The transverse mirror alignment was checked by simultaneous observation with a telescope of both the mirrors and the narrow part of vacuum chamber. Secondly, a preliminary angular adjustment of the mirrors was performed with the autocollimator, whose coincides with the axis of the narrow part of the vacuum chamber. Further angular adjustment was performed with an electron beam in the storage ring. Observing the electron beam position in the OK magnetic system through the same autocollimator, we put the beam on the optical axis. The angle at which the electrons enter the OK magnetic system was adjusted in such a way as to superpose the spontaneous radiation spot center with the center of an autocollimator objective. After such an alignment a red light spot was observed on the mirrors, which is typical for a slightly misaligned cavity. With an accurate alignment of the mirror angles we minimized the spot size, obtaining a bright point in the mirror center, about 1.5 cm in diameter for M1. With a X60 telescope focussed on the OK magnetic system we simultaneously observed the bright red beam of the light captured by the optical cavity and the slightly bluish electron beam. After final alignment the blue electron beam was in the center of the red light beam.

After alignment we measured the optical cavity losses. Prior to installing the mirrors in the vacuum chamber of the storage ring, their reflectances had been measured with a method we suggested, based upon damping time measurements for light in an optical cavity composed of the mirrors under study [7]. The measured coefficients are $K_1 = K_2 = 0.998$ at a wavelength $\lambda = 0.63$ μm. Optical cavity losses were measured during VEPP-3 operation using two diaphragms behind the front mirror (M1) (spaced by 10 m), an interference light filter (or monochromator) and a photomultiplier, as shown in fig. 6. An electron beam was kicked out using the single turn deflector, and the light signal damping was observed on an oscilloscope. In the beginning of the run the damping time was $\tau = 13$ μs, which is in a good agreement with the calculated value (for $K_{1,2} = 0.998$) $\tau = 15.6$ μs. By the end of the run the damping time had decreased to 5 μs. As shown by the direct measurements, this was caused by a decrease in the mirror reflectances (M1 – down to 0.991, M2 – down to 0.996). Such a degradation of mirror is apparently due to vacuum ultraviolet radiation on their surfaces.

To reach the lasing regime in the optical klystron, an exact synchronism of the light and electron bunches is necessary, and consequently the storage ring circumference should be multiple of the optical cavity length ($P = 8L$) to a high accuracy (~ 0.1 mm). For such an accuracy of alignment we could vary the electron revolution frequency in the storage ring by $\Delta f = 4$ kHz, corresponding to equilibrium orbit circumference changes of 74 mm. This change of an equilibrium orbit

is more convenient than the change of the distance between mirrors since it is more accurate, since it can be measured more accurately, and since it does not lead to optical cavity misalignment. The absence of transverse dispersion ($\eta = 0$, $\eta' = 0$) in the straight sections permits the electron beam coordinate and angle independence of the revolution frequency.

The alignment fixing $P = 8L$ was performed by two methods. The first method was to minimize the length of the light bunch captured in the optical cavity. Measurements of the light bunch length (its minimal length is the same as that of the electron bunch, $2l_{1/2} = 10$ cm) were performed with the stroboscopic method developed at our Institute, using an electron optical converter with transversely deflecting electrodes (dissector) [8]. Measurement accuracy of the bunch length is better than 1 cm, of the optical cavity length better than $\Delta L = (1 - K)l_{1/2} = 0.1$ mm. In the second method used the light passed through the diaphragms and the monochromator to the photomultiplier (as shown in fig. 6). The signal from the photomultiplier was applied to a phase detector whose reference signal was the output signal of the main generator of RF system of the storage ring VEPP-3, with a frequency of 16.12 MHz ($q = 4$). The output signal of the phase detector was measured with a digital voltmeter and then read into computer.

It is easy to show that the 4th harmonic amplitude varies with the intensity of the light coming from the optical cavity according to the following expression:

$$I = I_1 \exp[-i\varphi]$$
$$= I_0(\lambda)/(1 - K_1(\lambda)K_2(\lambda) \exp(4\pi i \Delta f/f_0)),$$

where $\Delta f/f_0 = (8L - P)/P$ and K_1 and K_2 are the mirror reflectances. Close to the resonance $4\pi\Delta f/f_0 < 1 - K_1 K_2$ we have the following $\varphi = 4\pi\Delta f f_0^{-1}(1 - K_1 K_2)^{-1}$. The phase measurement was performed at the position of the monochromator: at $\lambda_1 = \lambda_0 = 0.63$ μm and at $\lambda_2 = 0.45$ μm. At this wavelength the mirrors have a small reflectance $K_{1,2}(\lambda_2) \leqslant 0.3$. The phase dif-
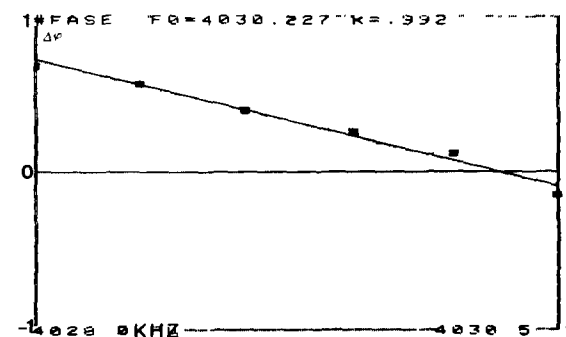

Fig. 4. The phase of the 4th harmonic of light intensity as a function of revolution frequency
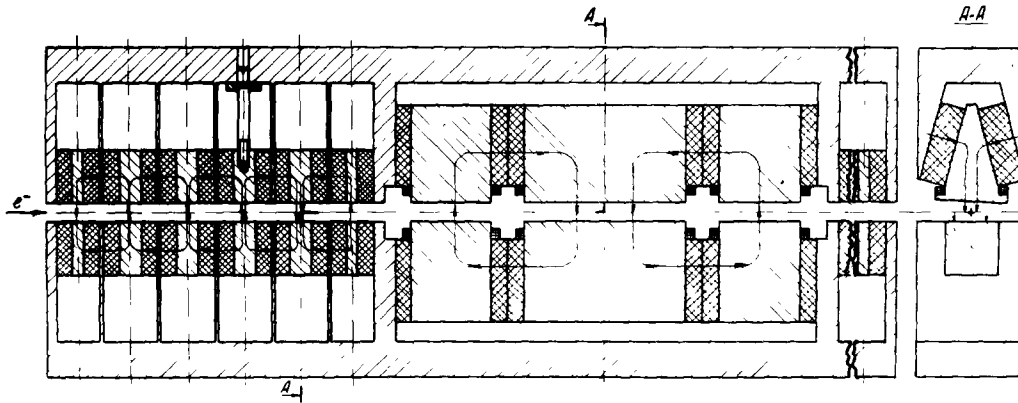
III. STORAGE RING FEL DEVICES

Fig. 5. The layout of the OK-2 magnetic system.

ference $\Delta\varphi = \varphi_1 - \varphi_2$ becomes zero at exact synchronism. The given method accuracy is $\Delta L \leqslant 30$ μm. Typical dependence $\Delta\varphi$ on the revolution frequency f is shown in fig. 4. The line slope also enables one to determine the cavity losses $(1 - K_1 K_2 = 4\pi\Delta f/f_0/\Delta\varphi)$. The results of these measurements coincide with the results of direct measurements of the damping time.

5. Magnetic system of the optical klystron

A detailed description of the OK-2 magnetic system is given in ref. [6]. The main parameters of the system are shown in table 2. A schematic diagram of the magnetic system is drawn in fig. 5.

6. Spontaneous radiation spectrum

The spontaneous radiation spectrum of the magnetic system of OK is the result of interference of radiation

Table 2
OK-2 and OK-3 magnetic system parameters

	OK-2	OK-3
Bunchers		
Total length (cm)	34	35
Maximum field (kG)	11	14
Pole width (cm)	4	6
Operational gap (cm)	1.1	1.3
Undulators		
Total length (cm)	2×33	2×82
Number of periods	2×4.5	2×11
Period (cm)	6.5	6.9
Magnetic field amplitude (kG)	7	6
Pole width (cm)	2 7	4
Operational gap (cm)	1.1	1.3–1.7

from two snakes:

$$I(\lambda) = 2I_0(\lambda)\left[1 + M \cos\left(\frac{2\pi\Delta s}{\lambda} + \varphi_0\right)\right], \qquad (2)$$

where λ is the wavelength, $I_0(\lambda)$ is the intensity of spontaneous radiation for each snake,

$$M = \exp\left[-\left(\frac{4\pi\Delta s}{\lambda}\frac{\sigma_E}{E}\right)^2/2\right]$$

is a modulation factor, σ_E/E is the relative energy spread of electrons, $\Delta s = e^2 H_b^2 L_b^3/96 E^2$ is the delay of electrons in the bunching section, H_b is the magnetic field and L_b is the buncher length. As is well known, the gain is proportional to the derivative over energy of the spontaneous radiation intensity at zero angle: $G \sim dI(\lambda)/dE$. This relation was derived theoretically both for the free electron laser [9] and for the more general case [2,10] including optical klystrons, and it was proven experimentally for two versions of magnetic systems [5,11]. Thus, by measuring the spontaneous radiation spectrum at zero angle we get the information on the optical klystron gain:

$$G_{\text{peak}} \sim \frac{\bar{I}}{\sigma_I}\frac{\Delta s}{\lambda} M \sin(2\pi\Delta s/\lambda + \varphi_0). \qquad (3)$$

where $\bar{I}$ is an electron current in the storage ring, and σ_I is the bunch length (for details see refs. [2,4]). An
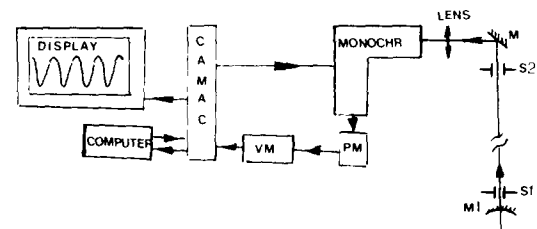

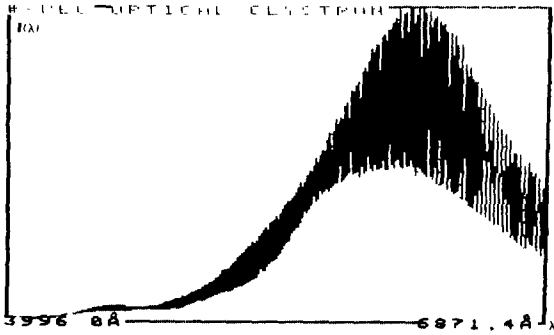Fig. 6. Spontaneous radiation spectrum measurement scheme.

Fig. 7. Spontaneous radiation spectrum for OK-2.

observation of the spectrum has been performed according to the scheme given in fig. 6. The light from the OK passed through the diaphragms and the monochromator to reach the photomultiplier. The computer controlled monochromator enabled us to perform a continuous scan within the given range of the wavelengths, with a step up to 0.5 A. The signal from the photomultiplier was measured with a digital voltmeter and read into a computer. The spontaneous radiation spectrum in the studied wavelength range and the modulation level M were displayed on the colour display within 10 s (see figs. 7 and 8). This enabled us to measure σ_E/E with the same method as a function of current, in agreement with (1) (see fig. 3). Thus, as follows from (1) and (3), the OK peak gain at large currents ($\sigma_E > 2\sigma_{E_0}$) is an universal function of the parameter $X = 4\pi\Delta s/\lambda(\bar{I}/I_0 \cdot V_{19}^{1/2}$ (kV))$^{1/2}$ and it reaches its maximum G_{max} at $X = 1$. In our calculations G_{max} is of 1.6–1.7%

$$G_{peak} = G_0 X \exp[-X^2/2].$$

To decrease the influence of the energy spread growth both on the spontaneous radiation spectrum and on the gain, one can use the OK bunching section with the field gradient ($\partial H_z/\partial x \neq 0$) [4,6,12]. This possibility was envisaged in the design of OK-2. By producing the field gradient $\partial H_z/\partial x$ in the dispersive section and
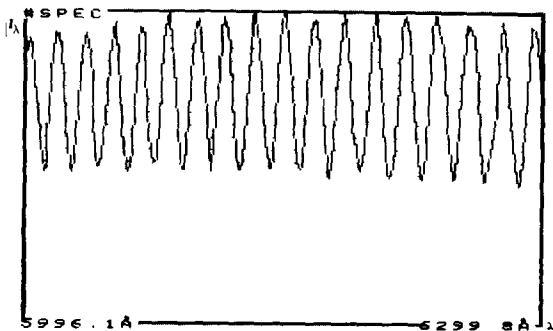
changing the storage ring lattice so that $\eta = 1$ m in the OK we cancelled the spontaneous radiation spectrum dependence on the electron energy. By varying the electron revolution frequency we observed that the spectrum shifted only on the edges of the frequency range, but always to the same side. Such a dependence can easily be explained by a nonhomogeneity of the field gradient in the buncher which is caused by the field distortion due to the vacuum chamber (see above). The spectrum modulation in this mode increased up to $M = 0.7$. Unfortunately, the field inhomogeneities in the buncher did not allow us to have acceptable current and beam lifetimes in this mode. Further work has been carried out in the mode $\eta = 0$ $\eta' = 0$ and $\partial H_z/\partial x = 0$. Nevertheless, we are now convinced of the operability of the buncher with a field gradient, and we are planning to use it in our new magnetic system of OK-3 (see below).

In spite of all the difficulties mentioned above we have observed the variation of the radiation spectrum under threshold. In the case of the optical cavity tuned below the generation threshold, some enhancement of the light captured into the cavity on the left-hand slopes of the spectrum ($dI/dK > 0$) with attenuation on the right-hand slopes ($dI/dK < 0$) is observed

$$I^*(\lambda) = 2I_0(\lambda)[1 + M \cos(2\pi\Delta s/\lambda + \varphi_0)]$$

$$\times \left[1 - (K_1K_2)^4\left(1 + G_{peak}(\bar{I}) \sin(2\pi\Delta s/\lambda + \varphi_0)\right)\right]^{-1}.$$

This leads to distortion of the radiation spectrum. The modulation spectrum phase depends on the gain, $\Delta\varphi \approx G_{peak}/G_{th}$ at $G_{peak} \ll G_{th}$. Fig. 9 shows the measurement results for φ versus the current. The maximum $\Delta\varphi$ measured was 0.3 ± 0.05. These measurements were performed at the end of the run when the reflectances had decreased so that G_{th} was 5% (compared to 1.6% at the beginning of the run). Consequently we have the peak gain per pass $G_{peak} = (1.5 \pm 0.2)\%$, which is in agreement with the calculated value. In order to avoid the

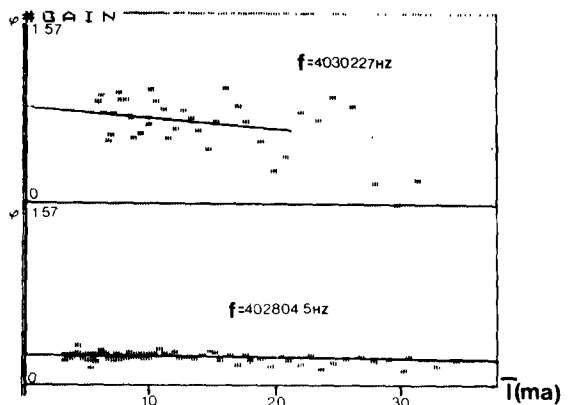Fig. 8. Fine structure of the spontaneous radiation spectrum.

Fig. 9. Spectrum modulation phase as a function of current.
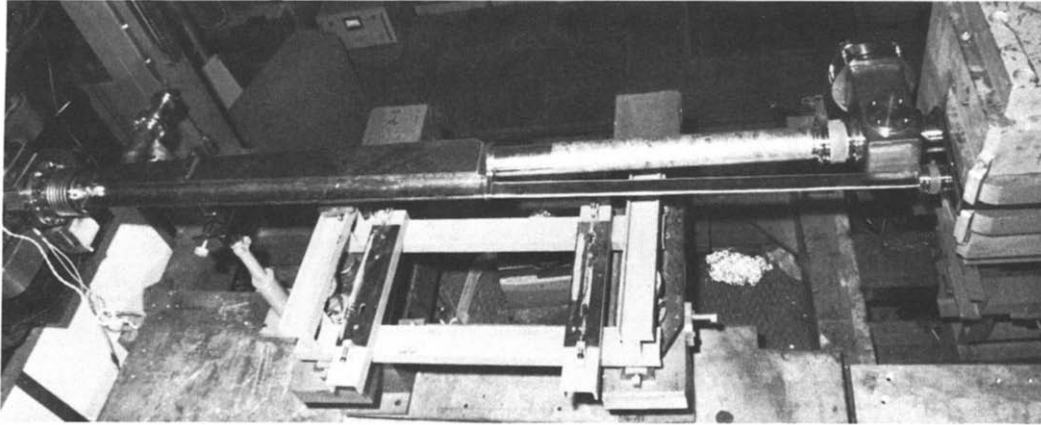
III. STORAGE RING FEL DEVICES

Fig. 10 The external view of the new vacuum chamber.

possibility of systematic errors we have repeated the same measurements at another revolution frequency ($P \neq 8L$). In these measurements φ did not depend on the current (see fig. 9).

7. New magnetic system for the OK and some future plans

At present, the new vacuum chamber with a large aperture (10 mm vertical, 40 mm horizontal) has been manufactured and installed in the storage ring VEPP-3. This enables installation of the OK magnetic system of 2 m total length. One half of the vacuum chamber has a cross section in the shape of a "key hole", and the other half consists of two separate tubes, i.e. it is a bypass (see fig. 10). With the OK operation the orbit passes through the bypass.

The OK-3 magnetic system consists of three separate sections: two undulators and the buncher. The new buncher is the compensated wiggler with three poles (see fig. 11). The magnetic field is produced with six coils connected in series. Each coil has four turns of water cooled busses with an effective cross section of 100 mm².

To ensure that the vertical magnetic field integral is zero we provide two correction coils (up and down). The buncher power supply is a 2.5 kA stabilized current source. The transverse field gradient, caused by a relative skew of the upper and lower parts of the dispersive
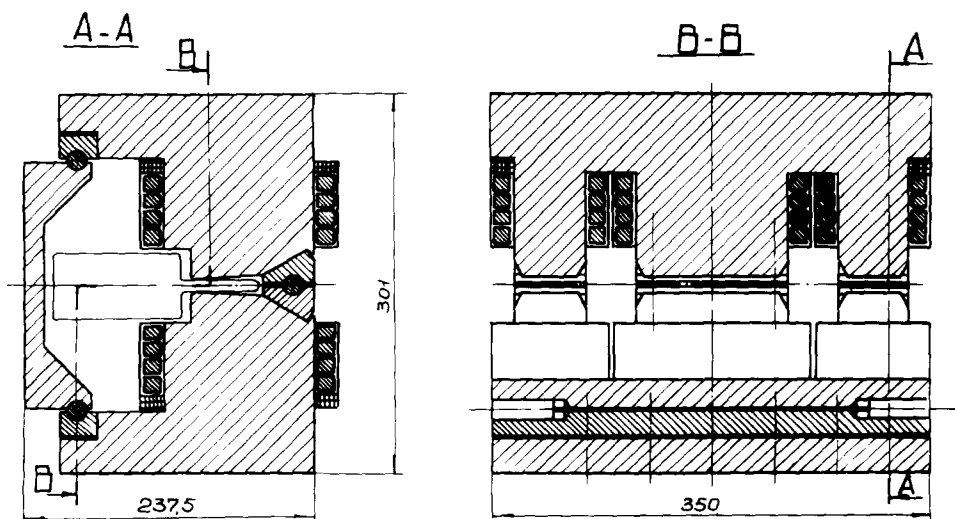

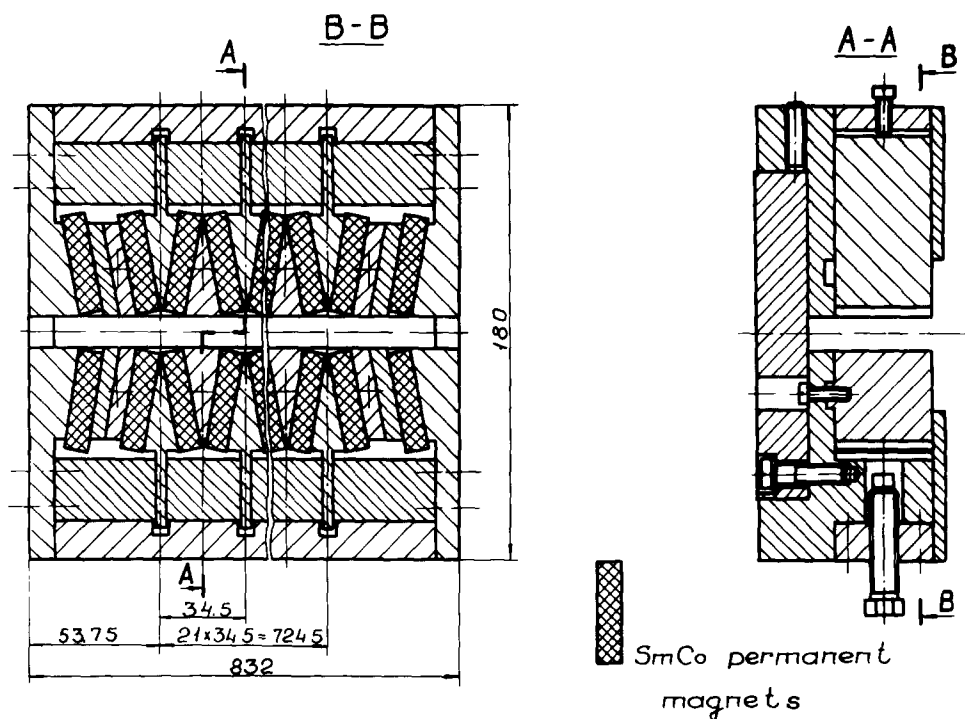Fig 11. The layout of the OK-3 buncher.

Fig. 12. The layout of OK-3 undulator.

section, is controlled by a special alignment screw. Some parameters of the buncher for OK-3 are given in table 2.

The OK-3 undulator design is given in fig. 12. In contrast to OK-2 the undulator poles are not rectangular, but have a wedge shape, lowering the stray field

Fig. 13. The OK-3 magnetic system installed on VEPP-3.

III. STORAGE RING FEL DEVICES

substantially. Iron screws in the upper and lower covers of the undulators are used for exact alignment of the field in each half-period, shunting magnetic flux from the operational aperture. Variation of the operational gaps in all the half periods of the undulator, in the range of 13 to 17 mm, are envisaged, for field control. The parameters of OK-2 and OK-3 undulators are given in table 2.

The OK-3 magnetic system installed on VEPP-3 is shown in fig. 13. According to the results of the first run with OK-3, we have chosen the transverse field gradient in the buncher corresponding to $(\partial \ln H_z/\partial x)^{-1} \approx 1.5$ m and the longitudinal dispersion corresponding to a 22 Å period of the spectrum fine structure at a wavelength of 6300 Å. We had a 7 A peak current and we suppose that the gain per pass was approximately 5%.

References

[1] N.A. Vinokurov and A.N. Skrinsky, Preprint INP 77-59, Novosibirsk (1977); N.A. Vinokurov, Proc. 10th Int. Conf. on High Energy Accelerators, vol. 2, Serpukhov (1977) p. 454.

[2] A.S. Artamonov et al., Nucl. Instr. and Meth. 177 (1980) 247.

[3] R. Coisson, Particle Accel. 11 (1981) 245; P. Elleaume, Physics of Quantum Electronics, vol. 8 (Addison Wesley, New York, Reading, 1982) ch. 5, p. 119.

[4] N.A. Vinokurov and A.N. Skrinsky, MW Relativistic Electronics (Gorky, 1981) p. 204.

[5] N.A. Vinokurov et al., Review of Synchrotron Radiation Applications in INP SD USSR Academy of Sciences (Novosibirsk, 1981) p. 12.

[6] G.A. Kornyukhin et al., Nucl. Instr. and Meth. 208 (1983) 189.

[7] N.A. Vinokurov and V.N. Litvinenko, Preprint INP 79-24, Novosibirsk (1979).

[8] E.I. Zinin, Nucl. Instr and Meth. 208 (1983) 439.

[9] A.A. Kolomensky and A.N. Lebedev, Proc. 10th Int. Conf. on High Energy Accelerators, vol. 2 (Serpukhov, 1977) p. 446; J.M.J. Madey, Nuovo Cim. 50 B (1979) 64.

[10] N.A. Vinokurov, Preprint INP 81-02, Novosibirsk (1981).

[11] L.R. Elias et al., Phys. Rev. Lett 36 (1976) 717; D.A.G Deacon et al., IEEE Trans. Nucl. Sci NS-29 (1981) 3142.

[12] N.A. Vinokurov and A.N. Skrinsky, Preprint INP 78-88, Novosibirsk (1978).

[13] N.A Vinokurov et al., Preprint INP 76-87, Novosibirsk (1976).